

Sergio Conti
Klaus Hackl *Editors*

Analysis and Computation of Microstructure in Finite Plasticity

Lecture Notes in Applied and Computational Mechanics

Volume 78

Series editors

Friedrich Pfeiffer, Technische Universität München, Garching, Germany
e-mail: pfeiffer@amm.mw.tum.de

Peter Wriggers, Universität Hannover, Hannover, Germany
e-mail: wriggers@ikm.uni-hannover.de

About this Series

This series aims to report new developments in applied and computational mechanics - quickly, informally and at a high level. This includes the fields of fluid, solid and structural mechanics, dynamics and control, and related disciplines. The applied methods can be of analytical, numerical and computational nature.

More information about this series at <http://www.springer.com/series/4623>

Sergio Conti · Klaus Hackl
Editors

Analysis and Computation of Microstructure in Finite Plasticity

 Springer

Editors

Sergio Conti
Inst. für Angewandte Mathematik
Universität Bonn
Bonn
Germany

Klaus Hackl
Lehrstuhl für Mechanik - Materialtheorie
Ruhr-Universität Bochum
Bochum
Germany

ISSN 1613-7736

ISSN 1860-0816 (electronic)

Lecture Notes in Applied and Computational Mechanics

ISBN 978-3-319-18241-4

ISBN 978-3-319-18242-1 (eBook)

DOI 10.1007/978-3-319-18242-1

Library of Congress Control Number: 2015937885

Springer Cham Heidelberg New York Dordrecht London

© Springer International Publishing Switzerland 2015

This work is subject to copyright. All rights are reserved by the Publisher, whether the whole or part of the material is concerned, specifically the rights of translation, reprinting, reuse of illustrations, recitation, broadcasting, reproduction on microfilms or in any other physical way, and transmission or information storage and retrieval, electronic adaptation, computer software, or by similar or dissimilar methodology now known or hereafter developed.

The use of general descriptive names, registered names, trademarks, service marks, etc. in this publication does not imply, even in the absence of a specific statement, that such names are exempt from the relevant protective laws and regulations and therefore free for general use.

The publisher, the authors and the editors are safe to assume that the advice and information in this book are believed to be true and accurate at the date of publication. Neither the publisher nor the authors or the editors give a warranty, express or implied, with respect to the material contained herein or for any errors or omissions that may have been made.

Printed on acid-free paper

Springer International Publishing AG Switzerland is part of Springer Science+Business Media
(www.springer.com)

Preface

The present volume presents research carried out within the research group FOR 797 “Analysis and computation of microstructure in finite plasticity” (*MICROPLAST*), financed by the German Science Foundation (DFG). The research group was established in 2007 and came to an end in 2015. During this period more than thirty researchers contributed actively to this endeavor, organized in eight sub-projects.

The aim of *MICROPLAST* was to understand and model dislocation based microstructure formation and evolution in materials, and develop tools to compute it effectively. This is important because plasticity determines a number of industrial and natural phenomena, ranging from the deformation of the earth crust to forming of metals. Most plastic processes are strongly influenced by the formation and evolution of dislocation patterns and other plastic microstructures. Classical plasticity models were able to make useful predictions without accounting for the microstructure, and focusing on a phenomenological understanding of the macroscopic material response. These models have, however, strong limitations, concerning in particular the transferability of the results, the applicability to large deformations, to small samples, and the treatment of ageing and fatigue.

The foundation of *MICROPLAST* was inspired both by new mathematical and modeling developments and by new experimental techniques. Around the turn of the millennium novel variational concepts became available allowing to formulate finite plasticity and associated microstructure formation within a rigorous and powerful mathematical framework. The systematic variational formulation of the evolution of internal variables via dissipation potentials and dissipation distances made it possible to apply the concepts of relaxation theory and Γ -convergence, that were originally developed for static problems, to the evolution of inelastic materials.

At the same time experimental techniques had advanced to a stage where it became possible to perform in situ measurements of dislocation microstructures and their evolution, thus giving valuable information for the development of the corresponding models. For this reason, *MICROPLAST* was established as an interdisciplinary cooperation of scientists from the fields of mathematics, mechanics and materials sciences, working closely together on a common goal.

This volume contains reports on the various achievements reached within *MICROPLAST*. These range from experimental evidence on the mechanisms of microstructure formation to micromechanical and multiscale models of these processes. They include derivations of relaxed envelopes of non-convex energies using novel developments of variational calculus, as well as full mathematical analysis of the models established, and the development of suitable and fast numerical schemes.

It is our hope that we succeeded in giving an insight into a new developing field, and that the readers will find the material in this volume interesting and beneficial for their research.

The contributions in this volume have undergone an internal peer-review. We are convinced that this process led to significant improvements in the papers contained in this book.

Finally, we would like to thank the German Science Foundation for their generous support and the always very pleasant and professional cooperation.

April 2015

Sergio Conti
Klaus Hackl

MICROPLAST

Contents

1 Numerical Algorithms for the Simulation of Finite Plasticity with Microstructures	1
<i>Carsten Carstensen, Dietmar Gallistl, Boris Krämer</i>	
1.1 Introduction	1
1.2 Preliminaries and Notation	3
1.3 Convergent Adaptive Finite Element Method for the Two-Well Problem in Elasticity	4
1.3.1 Review of the Model Problem	5
1.3.2 Adaptive Algorithm	6
1.3.3 Convergence for the Deformation Gradient	9
1.4 Guaranteed Lower Energy Bounds for the Two-Well Problem	10
1.4.1 Nonconforming FEM and Discrete Energy Functional	10
1.4.2 Lower Energy Bounds	12
1.4.3 Guaranteed Error Control for the Pseudo-stress	15
1.4.4 Numerical Experiments	16
1.5 Discontinuous Galerkin Method for Degenerate Convex Minimization Problems	17
1.5.1 Optimal Design Benchmark	18
1.5.2 Discontinuous Galerkin Methods	20
1.5.3 Lifting Operator R	20
1.5.4 Connection with the Nonconforming Method	21
1.5.5 Adaptive Finite Element Method	22
1.5.6 Computational Experiments	22
1.5.7 Γ -shaped Domain	23
1.5.8 Slit Domain	24
1.6 Conclusions and Outlook	25

2 Variational Modeling of Slip: From Crystal Plasticity to Geological Strata	31
<i>Sergio Conti, Georg Dolzmann, Carolin Kreisbeck</i>	
2.1 Introduction	31
2.2 Experimental Observation of Slip Microstructures in Nature	33
2.2.1 Chevron Folds in Rocks	34
2.2.2 Kink Bands in Stacks of Paper under Compression	34
2.2.3 Simple Laminates in Shear Experiments in Crystal Plasticity	36
2.3 The Hunt-Peletier-Wadee Model for Kink Bands	37
2.4 Variational Modeling of Microstructure	38
2.5 Models in Crystal Plasticity with One Active Slip System	41
2.5.1 Variational Formulation of Crystal Plasticity	42
2.5.2 Relaxation Results in Crystal Plasticity with One Slip System	44
2.5.3 Heuristic Origin of the Laminates	46
2.5.4 Relation to Kink Bands in Rocks	49
2.5.5 Elastic Approximation	51
2.5.6 Higher-Order Regularizations	52
2.6 Beyond One Slip-System	53
2.6.1 Two Slip Systems in a Plane	53
2.6.2 Three Slip Systems in a Plane	54
3 Rate-Independent versus Viscous Evolution of Laminate Microstructures in Finite Crystal Plasticity	63
<i>Christina Günther, Dennis M. Kochmann, Klaus Hackl</i>	
3.1 Introduction	63
3.2 Variational Modeling of Microstructures	64
3.3 Single Slip Crystal Plasticity	67
3.4 Partial Analytical Relaxation via Lamination	67
3.5 Rate-Independent Evolution	70
3.5.1 Evolution Equations	70
3.5.2 Laminate Rotation	71
3.5.3 Laminate Initiation	72
3.5.4 Numerical Scheme	72
3.6 Simulation of Rotating Laminates	73
3.7 Viscous Evolution	75
3.7.1 Evolution Equations	76
3.7.2 Laminate Rotation	77
3.7.3 Laminate Initiation	77
3.8 Comparison of the Laminate Evolution for the Rate-Independent Case and the Viscosity Limit	78
3.9 Conclusion and Discussion	85

4	Variational Gradient Plasticity: Local-Global Updates, Regularization and Laminate Microstructures in Single Crystals	89
	<i>Steffen Mauthe, Christian Miehe</i>	
4.1	Introduction	90
4.2	A Multifield Formulation of Gradient Crystal Plasticity	93
4.2.1	Introduction of Long-Range Field Variables	93
4.2.2	Introduction of Short-Range Field Variables	96
4.2.3	Energy Storage, Dissipation Potential and Load Functionals	99
4.2.4	Rate-Type Variational Principle and Euler Equations . . .	102
4.2.5	Explicit Form of the Micro-force Balance Equations . . .	103
4.3	Algorithmic Formulation of Gradient Crystal Plasticity	103
4.3.1	Time-Discrete Field Variables in Incremental Setting . . .	103
4.3.2	Update Algorithms for the Short-Range Field Variables	104
4.3.3	Time-Discrete Incremental Variational Principle	105
4.3.4	Space-Time-Discrete Incremental Variational Principle	106
4.4	Example 1: Analysis of an F.C.C. Crystal Grain Aggregate	108
4.4.1	Slip Systems and Euler Angles	108
4.4.2	Voronoi-Tessellated Unit Cell under Shear	109
4.5	Example 2: Laminate Microstructure in Single Crystals	110
4.5.1	Double Slip Systems	111
4.5.2	Implications of Same Plane Double Slip	112
4.5.3	Laminate Deformation Microstructure in Single Crystal Copper	114
4.6	Conclusion	118
5	Variational Approaches and Methods for Dissipative Material Models with Multiple Scales	125
	<i>Alexander Mielke</i>	
5.1	Introduction	125
5.2	Variational Formulations for Evolution	127
5.2.1	Generalized Gradient Systems and the Energy-Dissipation Principle	128
5.2.2	Rate-Independent Systems and Energetic Solutions	132
5.3	Evolutionary Γ -Convergence	134
5.3.1	pE-convergence for Generalized Gradient Systems	134
5.3.2	pE-convergence for Rate-Independent Systems	137
5.4	Justification of Rate-Independent Models	138
5.4.1	Wiggly Energies Give Rise to Rate-Independent Friction	139
5.4.2	1D Elastoplasticity as Limit of a Chain of Bistable Springs	141

5.4.3	Balanced-Viscosity Solutions as Vanishing-Viscosity Limits	143
5.5	Rate-Independent Evolution of Microstructures	147
5.5.1	Laminate Evolution in Finite-Strain Plasticity	148
5.5.2	A Two-Phase Shape-Memory Model for Small Strains	149
6	Energy Estimates, Relaxation, and Existence for Strain-Gradient Plasticity with Cross-Hardening	157
	<i>Keith Anguige and Patrick W. Dondl</i>	
6.1	Introduction	158
6.2	A Continuum Model for Strain-Gradient Plasticity with Cross Hardening	159
6.2.1	Plastic Shear	160
6.2.2	Locks and Cross-Hardening	161
6.2.3	Geometrically Necessary Dislocations	162
6.2.4	The Model	163
6.3	Relaxation of the Single-Slip Condition	164
6.4	Some Remarks about Existence of Minimizers	168
6.5	Energy Estimates for a Shear Experiment	168
6.6	Conclusions	171
7	Gradient Theory for Geometrically Nonlinear Plasticity via the Homogenization of Dislocations	175
	<i>Stefan Müller, Lucia Scardia, Caterina Ida Zeppieri</i>	
7.1	Introduction	175
7.2	Key Mathematical Challenges	183
7.3	Heuristics for Scaling Regimes	184
7.3.1	The Core Energy of a Single Dislocation	184
7.3.2	The Core Energy of Many Dislocations	186
7.3.3	The Interaction Energy	187
7.4	Main Result	189
7.4.1	Set-Up	189
7.4.2	Results	191
7.5	Ideas of Proof	193
8	Microstructure in Plasticity, a Comparison between Theory and Experiment	205
	<i>Olga Dmitrieva, Dierk Raabe, Stefan Müller, and Patrick W. Dondl</i>	
8.1	Introduction	205
8.2	Modeling Continuum Plasticity	207
8.3	A Single-Pass Shear Deformation Experiment and the Resulting Microstructure	208
8.3.1	Sample Preparation and Shear Deformation Experiments	208

8.3.2	Digital Image Correlation for Strain Mapping and EBSD for Texture Mapping	209
8.3.3	Outcome of the Single Crystal Shear Deformation Experiments	210
8.3.4	Energy Minimizing Microstructure	212
8.3.5	An Analysis of the Substructure Within the Lamination Bands	215
8.4	Conclusions	216
9	Construction of Statistically Similar RVEs	219
	<i>Lisa Scheunemann, Daniel Balzani, Dominik Brands, Jörg Schröder</i>	
9.1	Introduction	220
9.2	Statistically Similar RVEs	222
9.2.1	Method	223
9.2.2	Lower and Upper Bounds of RVEs	224
9.2.3	Statistical Measures	225
9.3	Construction and Analysis of SSRVEs	233
9.3.1	Objective Functions	235
9.3.2	Coupled Micro-macro Simulations	240
9.3.3	SSRVEs Based on Different Sets of Statistical Measures	241
9.3.4	Comparison of Stress on Microscale	244
9.3.5	Analysis of Bounds	248
9.4	Conclusion	250
	Author Index	257

Chapter 1

Numerical Algorithms for the Simulation of Finite Plasticity with Microstructures

Carsten Carstensen, Dietmar Gallistl, and Boris Krämer

Abstract. This article reports on recent developments in the analysis of finite element methods for nonlinear PDEs with enforced microstructures. The first part studies the convergence of an adaptive finite element scheme for the two-well problem in elasticity. The analysis is based on the relaxation of the classical model energy by its quasiconvex envelope. The second part aims at the computation of *guaranteed lower energy bounds* for the two-well problem with nonconforming finite element methods that involve a stabilization for the discrete linear Green strain tensor. The third part of the paper investigates an adaptive discontinuous Galerkin method for a degenerate convex problem from topology optimization and establishes some equivalence to nonconforming finite element schemes.

1.1 Introduction

Mathematical models in the framework of nonlinear elasticity for phase transformations in solids [BJ87, CK88, BJ92] and for elastoplastic deformations [CHM02] lead to variational problems for which the existence of minimizers cannot be obtained by the direct method in the calculus of variations, for further applications and references see [CDK11, CDK13, CDK15] and the literature quoted therein.

Carsten Carstensen
Humboldt-Universität zu Berlin, Institut für Mathematik,
Unter den Linden 6, D-10099 Berlin, Germany
e-mail: cc@math.hu-berlin.de

Dietmar Gallistl
Universität Bonn, Institut für Numerische Simulation,
Wegelerstraße 6, D-53115 Bonn, Germany
e-mail: gallistl@ins.uni-bonn.de

Boris Krämer
Humboldt-Universität zu Berlin, Institut für Mathematik,
Unter den Linden 6, D-10099 Berlin, Germany
e-mail: kraemer@math.hu-berlin.de

The infimization of the energy enforces oscillations of the infimizing sequence on finer and finer scales called microstructures and converge only weakly but not strongly. Typically the weak limit is not a minimizer of the original minimization problem and has to be replaced by a generalized minimizer which involves the gradient Young measure associated to the sequence of deformation gradients [KP91, MŠ99].

The numerical simulation of problems of this kind is an ongoing challenging task and a direct minimization of the nonconvex energy in a finite element space leads to strongly mesh-dependent effects [Lus96, Chi00, Car01]. An alternative approach is based on a minimization of the relaxed variational problem [Dac08] obtained by replacing the energy density W by its quasiconvex relaxation W^{qc} , that is, one minimizes

$$I^{\text{qc}}(v) := \int_{\Omega} W^{\text{qc}}(\varepsilon(v)) dx - \int_{\Omega} f \cdot v dx \quad \text{among all } v \text{ in } \mathcal{A} := u_D + H_0^1(\Omega; \mathbb{R}^2). \quad (1.1)$$

Here the function $u_D \in H^1(\Omega; \mathbb{R}^2)$ defines the Dirichlet boundary conditions for the problem and the linear Green strain $\varepsilon(v)$ is the symmetric part of the deformation gradient Du . Since the energy density in the relaxed minimization problem satisfies the necessary convexity conditions in the vector-valued calculus of variations, problem (1.1) allows for a minimizer in \mathcal{A} . Moreover, any minimizer u characterizes a macroscopic deformation of the original problem in the sense that there exists a sequence $(u_j)_{j \in \mathbb{N}}$ which infimizes the energy of the original variational problem and converges weakly to u . If this convergence is also strong in $H^1(\Omega; \mathbb{R}^2)$, then the minimum of the energy is attained and u is a classical minimizer of the original problem.

This approach is extremely appealing, if an explicit formula for W^{qc} is known. In this case one can construct for a given deformation gradient F , a corresponding gradient Young measure ν with center of mass F which realizes the relaxed energy, $W^{\text{qc}}(F) := \langle \nu, W \rangle := \int_{\mathbb{R}^{2 \times 2}} W(F) d\nu(F)$, and provides at the same time a representation for the stress variable $\sigma(F) = DW^{\text{qc}}(F) := \langle \nu, DW \rangle := \int_{\mathbb{R}^{2 \times 2}} DW(F) d\nu(F)$; see [BKK00] and [CM02] for a discussion of the regularity of the stress variable. In this way one obtains the associated stresses which are of fundamental importance in engineering applications. A successful example of this approach in the numerical analysis of a relaxed problem can be found in [CP97, CP01].

A posteriori error estimation for relaxed nonconvex problems or degenerate convex problems typically encounters the reliability-efficiency gap [CJ03]. This means that reliable a posteriori error estimators converge with a worse rate compared to the true error and, hence, is not efficient: The efficiency index even diverges towards ∞ .

The motivation of effective numerical simulations of microstructures in finite plasticity arose in [CHM02], where it is shown that a typical time-step in finite plasticity leads to a non convex minimization problem and that shear bands may be seen as microstructures in the corresponding minimization process. The relaxation models in the post-modern calculus of variations [Dac08] appears as the only feasible approach for a computer simulation in [Car01] and this provoked massive

research on relaxation models of single- and multiple-slip systems and their time evolution in this research group. The numerical treatment needs an extra justification and, even if some convergence analysis arises naturally in [CP97] for a class of convexified model problems, there remain severe open questions in the adaptive mesh-refining [Car08] and in efficient and reliable error control [CJ03]. The mathematical understanding of the performance of the related discretization schemes could not follow the lines of an implicit function theorem [CD04] because of the too restrictive smallness and uniform polyconvexity assumptions. The latter at least seemingly contradicts the concept of a related hull in finite plasticity. The research of this project therefore started at the understanding of the convexified model problems of [CM02, CP97, Car08] and their generalization to polyconvex problems with standard [CP97, Car08] and nonstandard discretization [CGR12] and a focus on adaptive mesh-refining with a complete a priori and posterior error analysis.

In the first part of this paper, we outline the convergence analysis for the relaxation of the classical model energy in a two-dimensional setting for which the relaxation was obtained in [Koh91, LC88, Pip91]; see (1.6) below for the precise formula. From the point of view of numerical analysis, one striking advantage of the relaxed minimization problem is that the macroscopic deformation u can, in principle, be computed with a strongly convergent sequence of minimizers in suitable finite element spaces. The reliability-efficiency gap does not prevent the convergence proof of the associated stresses for a large class of variational problems with energy densities that fail to be strictly convex [Car08].

The second part of this paper is devoted to the computation of *guaranteed lower energy bounds* for the two-well problem of [Koh91, LC88, Pip91]. The nonconforming finite element method serves as the main tool for deriving those lower bounds.

In the third part of the paper, we investigate a discontinuous Galerkin method for a degenerate convex problem from topology optimization. The reliability-efficiency gap motivated stabilized finite element methods (FEMs) [BC10, BC14] for degenerate convex minimization problems. The recent developments of [CL15] could improve the reliability-efficiency gap with duality methods and nonconforming FEMs. The discontinuous Galerkin method here appears as a natural choice of a stabilized discontinuous method and this paper succeeds in establishing an equivalence to a nonconforming finite element method. The conclusion in Section 1.6 connects the research in this project with the achievements of this research group and contains various open questions for future research.

1.2 Preliminaries and Notation

Let $\Omega \subseteq \mathbb{R}^2$ be a bounded polygonal Lipschitz domain with outer unit normal ν along the boundary $\partial\Omega$. Let \mathcal{T} be a regular triangulation of Ω into triangles in the sense of Ciarlet, with edges \mathcal{F} and vertices \mathcal{N} . The interior (resp. boundary) edges are denoted by $\mathcal{F}(\Omega)$ (resp. $\mathcal{F}(\partial\Omega)$). Analogously let $\mathcal{N}(\Omega)$ denote the interior vertices and $\mathcal{N}(\partial\Omega)$ denote the vertices on the boundary. The set of edges of a triangle $T \in \mathcal{T}$ reads $\mathcal{F}(T)$, the set of vertices of T is denoted by $\mathcal{N}(T)$. For any

$T \in \mathcal{T}$ let $h_T = \text{diam}(T)$ and define the piecewise constant mesh-size function $h_{\mathcal{T}}$ by $h_{\mathcal{T}}|_T := h_T$. The length of an edge $F \in \mathcal{F}$ is denoted by h_F . For any interior edge $F \in \mathcal{F}(\Omega)$, there exist two adjacent triangles T_+ and T_- such that $F = \partial T_+ \cap \partial T_-$. Let $\mathbf{v}_F = (\mathbf{v}_F(1); \mathbf{v}_F(2))$ denote the fixed normal vector of F that points from T_+ to T_- . For $F \in \mathcal{F}(\partial\Omega)$, let \mathbf{v}_F denote the outward unit normal vector of Ω . The tangential vector of an edge F is denoted by $\boldsymbol{\tau}_F := (-\mathbf{v}_F(2); \mathbf{v}_F(1))$. Given any (possibly vector-valued) function v , define the jump and the average of v of across $F \in \mathcal{F}(\Omega)$ by

$$[v]_F := v|_{T_+} - v|_{T_-} \quad \text{and} \quad \langle v \rangle_F := (v|_{T_+} + v|_{T_-})/2 \quad \text{along } F.$$

For a boundary edge $F \in \mathcal{F}(\partial\Omega) \cap \mathcal{F}(T_+)$, define $[v]_F := v|_F - u_D|_F$ and $\langle v \rangle_F := (v|_F + u_D|_F)/2$ for the prescribed Dirichlet data u_D .

For any $T \in \mathcal{T}$, the space of polynomial functions of degree at most k is denoted by $P_k(T)$. The space of piecewise polynomials reads

$$P_k(\mathcal{T}) = \{v \in L^2(\Omega) \mid \forall T \in \mathcal{T}, v|_T \in P_k(T)\}.$$

The piecewise action of the derivative D is denoted by D_{nc} . The symmetric part of the gradient reads $\varepsilon := \text{sym}D$ and its piecewise action reads ε_{nc} . The L^2 projection onto piecewise constants with respect to \mathcal{T} is denoted by Π_0 .

Standard notation on Lebesgue and Sobolev spaces applies throughout this paper; $H^{-1}(\Omega)$ denotes the dual spaces of $H_0^1(\Omega)$. The space of smooth functions with compact support in Ω is denoted by $\mathcal{D}(\Omega)$. The L^2 norm over the domain Ω is abbreviated as $\|\cdot\| := \|\cdot\|_{L^2(\Omega)}$. The L^2 inner product reads $(\cdot, \cdot)_{L^2(\Omega)}$. The integral mean is denoted by \bar{f} . The space of real 2×2 matrices reads $\mathbb{M} \equiv \mathbb{R}^{2 \times 2}$. The symmetric part of a matrix $A \in \mathbb{M}$ reads $\text{sym}A$. The space of symmetric 2×2 matrices reads $\mathbb{S} := \text{sym}\mathbb{M}$. The dot denotes the product of two one-dimensional lists of the same length while the colon denotes the Euclidean product of matrices, e.g., $a \cdot b = a^\top b \in \mathbb{R}$ for $a, b \in \mathbb{R}^2$ and $A : B = \sum_{j,k=1}^2 A_{jk} B_{jk}$ for 2×2 matrices A, B . The measure $|\cdot|$ is context-sensitive and refers to the number of elements of some finite set or the length of an edge or the area of some domain and not just the modulus of a real number or the Euclidean length of a vector.

1.3 Convergent Adaptive Finite Element Method for the Two-Well Problem in Elasticity

In this section we outline the convergence analysis for the relaxation of the classical model energy

$$W(E) = \min \left\{ \frac{1}{2} \langle \mathbb{C}(E - A_1), E - A_1 \rangle + w_1, \frac{1}{2} \langle \mathbb{C}(E - A_2), E - A_2 \rangle + w_2 \right\} \quad (1.2)$$

in a two-dimensional setting for which the relaxation was obtained in [Koh91, LC88, Pip91]. see (1.6) below for the precise formula with given symmetric matrices A_1

and A_2 called the wells. It turns out that the quasiconvex relaxation is in fact the convex relaxation if and only if the two preferred strains A_1 and A_2 are compatible, see [Koh91, Lemma 4.1] for necessary and sufficient conditions for compatibility. The case of compatible wells was analyzed in [Car08] and therefore we focus on the incompatible case in this paper. Moreover, we assume that the matrix $A_1 - A_2$ is not proportional to the identity matrix since in this case the uniqueness of minimizers may be lost [Ser96, Remark 2.2]. Hence we assume that the eigenvalues η_1 and η_2 of the matrix $A_1 - A_2$ satisfy

$$0 < \eta_1 < \eta_2. \quad (1.3)$$

We refer to the problem as nonconvex since for incompatible wells the relaxation is not convex but quasiconvex.

1.3.1 Review of the Model Problem

In this subsection, we recall the model two-well problem following the discussion in [CD14]. The starting point is the nonconvex energy density W for a two-dimensional model in linear elasticity with linear kinematics for a phase transforming material with two preferred elastic strains A_1 and $A_2 \in \mathbb{S}$ and elasticity tensor \mathbb{C} for which

$$W(E) := \min\{W_1(E), W_2(E)\} \quad \text{for all } E \in \mathbb{S} \quad (1.4)$$

with suitable constants $w_j \in \mathbb{R}$ and

$$W_j(E) := \frac{1}{2} \langle \mathbb{C}(E - A_j), E - A_j \rangle + w_j \quad \text{for } j = 1, 2. \quad (1.5)$$

The focus lies on the classical case of an isotropic Hooke's law with bulk modulus $\kappa > 0$ and shear modulus $\mu > 0$, i.e.,

$$\mathbb{C}E := \kappa(\text{tr}E)1_{2 \times 2} + 2\mu \text{dev}E \quad \text{for any } E \in \text{sym}\mathbb{M} \equiv \mathbb{S}.$$

Since A_1 and A_2 are symmetric matrices, we may relabel the matrices in such a way that the eigenvalues η_1 and η_2 of $A_1 - A_2$ satisfy $\eta_1 \geq |\eta_2|$ and, after a suitable change of coordinates, we may suppose that the eigenvectors are parallel to the coordinate axes, i.e., $A_1 - A_2 = \text{diag}(\eta_1, \eta_2)$. It is well-established (see, e.g., Lemma 4.1 in [Koh91]) that A_1 and A_2 are incompatible as linear elastic strains if and only if $\eta_2 > 0$. The relaxed energy density W^{qc} was computed by Kohn [Koh91], Lurie and Cherkashev [LC88], and Pipkin [Pip91]. As mentioned, e.g., in [Koh91], Section 4, the relaxation is piecewise quadratic and globally C^1 , and in the notation of this reference given by the expression below. Define $\nu := (\kappa - \mu)/\mu$ as well as (for $j = 1, 2$)

$$\gamma_j := (\kappa - \mu) \operatorname{tr}(A_1 - A_2) + 2\mu \eta_j \quad \text{and} \quad g := \frac{\gamma_1^2}{\kappa + \mu} = \frac{\gamma_1^2}{\mu(\mu + 2)}.$$

Let

$$\begin{aligned} \mathcal{P}_1 &= \{E \in \mathbb{S} \mid W_1(E) - W_2(E) + g/2 \leq 0\}, \\ \mathcal{P}_2 &= \{E \in \mathbb{S} \mid W_1(E) - W_2(E) - g/2 \geq 0\}, \\ \mathcal{P}_{\text{rel}} &= \{E \in \mathbb{S} \mid |W_1(E) - W_2(E)| \leq g/2\}. \end{aligned}$$

The quasiconvex envelope of W [Koh91, Pip91, LC88] reads

$$W^{\text{qc}}(E) = \begin{cases} W_1(E) & \text{if } E \in \mathcal{P}_1, \\ W_2(E) & \text{if } E \in \mathcal{P}_2, \\ W_2(E) - \frac{1}{2g}(W_2(E) - W_1(E) + g/2)^2 & \text{if } E \in \mathcal{P}_{\text{rel}} \end{cases} \quad (1.6)$$

for any $E \in \mathbb{S}$. This gives rise to the macroscopic energy

$$I^{\text{qc}}(v) := \int_{\Omega} W^{\text{qc}}(\varepsilon(v)) dx - \int_{\Omega} f \cdot v dx. \quad (1.7)$$

Let

$$\gamma := \mu(\tilde{\nu} - (\tilde{\nu} + 2)\gamma_2/\gamma_1) \quad \text{for} \quad \tilde{\nu} := (\kappa - \mu)/\mu. \quad (1.8)$$

The translated energy utilizes the shifted energy density

$$\Phi(X) = W^{\text{qc}}(\operatorname{sym} X) - \gamma \det X \quad \text{for any } X \in \mathbb{M} \quad (1.9)$$

and amounts to

$$E(v) := \int_{\Omega} \Phi(Dv) dx - \int_{\Omega} f \cdot v dx \quad \text{for any } v \in \mathcal{A}.$$

It turns out [CD14] that this convex functional has (possibly non-unique) minimizers in $u \in \mathcal{A}$ which lead to a unique pseudostress $\tau := D\Phi(Du)$.

1.3.2 Adaptive Algorithm

This section describes an algorithm for adaptive mesh-refining. The following paragraphs are (in parts) a repetition of material published in [CD14].

Given an initial shape-regular triangulation \mathcal{T}_0 , this scheme generates a sequence of triangulations \mathcal{T}_ℓ and corresponding finite element spaces $V^{(\ell)}$ which are shape-regular depending on the initial configuration. In particular, all constants are independent of ℓ .

1.3.2.1 INPUT

The input required by the numerical scheme is a shape-regular triangulation \mathcal{T}_0 of the bounded domain $\Omega \subset \mathbb{R}^2$, the associated finite element space $V^{(0)} = V(\mathcal{T}_0)$ of continuous functions which are on all elements affine polynomials with values in \mathbb{R}^2 , and a fixed parameter Θ with $0 < \Theta < 1$ for the marking strategy. For simplicity, we assume that the Dirichlet condition u_D is contained in $V^{(0)}$.

1.3.2.2 SOLVE and the Discrete Minimization Problems

Given the triangulation \mathcal{T}_ℓ , $\ell \in \mathbb{N}_0$, with the corresponding discrete spaces $V^{(\ell)} = V(\mathcal{T}_\ell)$ and $V_0^{(\ell)} = V_0(\mathcal{T}_\ell)$ on the level ℓ , compute the discrete solution $u_\ell \in u_D + V_0^{(\ell)} \equiv \mathcal{A}_\ell$ as the unique minimizer of the energy functional I^{qc} on \mathcal{A}_ℓ . For simplicity, we suppose that the discrete solution is computed exactly. Then, the discrete stress is given by

$$\sigma_\ell = DW^{\text{qc}}(\varepsilon(u_\ell)) \in L^2(\mathcal{T}_\ell; \mathbb{S}).$$

Note that DW^{qc} is piecewise affine and globally continuous and hence globally Lipschitz continuous. Since $\varepsilon(u_\ell) \in P_0(\mathcal{T}_\ell; \mathbb{S})$ is piecewise constant, so is $\sigma_\ell \in L^2(\mathcal{T}_\ell; \mathbb{S})$.

1.3.2.3 ESTIMATE

Suppose that T_+ and T_- are two distinct triangles in \mathcal{T}_ℓ with a common edge $F = \partial T_+ \cap \partial T_- \in \mathcal{F}_\ell(\Omega)$ of length $|F|$. The unit normal vector

$$\mathbf{v}_F = \mathbf{v}_{T_+}|_F = -\mathbf{v}_{T_-}|_F \quad \text{along } F$$

is defined up to the orientation which we fix as the orientation of the outer normal \mathbf{v}_{T_+} of T_+ along F . Given the discrete stress $\sigma_\ell = DW^{\text{qc}}(\varepsilon(u_\ell)) \in L^2(\mathcal{T}_\ell; \mathbb{S})$ of the previous subsection, the jump of σ_ℓ across the edge is defined as

$$[\sigma_\ell]_F \mathbf{v}_F = \sigma_\ell|_{T_+} \mathbf{v}_{T_+} + \sigma_\ell|_{T_-} \mathbf{v}_{T_-} = (\sigma_\ell|_{T_+} - \sigma_\ell|_{T_-}) \mathbf{v}_F \quad \text{along } F.$$

Let $\mathcal{F}(T)$ denote the set of the three edges of a triangle $T \in \mathcal{T}_\ell$ and $\mathcal{F}_{\text{int}}(T) = \mathcal{F}(T) \setminus \mathcal{F}_\ell(\partial\Omega)$ the subset of interior edges. To each triangle $T \in \mathcal{T}_\ell$ with area $|T|$ we associate the error estimator contribution $\eta_\ell(T)$ given by

$$\eta_\ell^2(T) = |T| \|f + \text{div} \sigma_\ell\|_{L^2(T)}^2 + |T|^{1/2} \sum_{F \in \mathcal{F}_{\text{int}}(T)} \|[\sigma_\ell]_F \mathbf{v}_F\|_{L^2(F)}^2.$$

The sum

$$\eta_\ell^2 = \sum_{T \in \mathcal{T}_\ell} \eta_\ell^2(T)$$

is indeed an error estimator for the accompanying pseudo-stress approximations from the translated energy minimization problem, see [CD14]. However, the upper bound η_ℓ of the pseudo-stress error is not sharp, the reliable error estimator η_ℓ is not

efficient. This dramatic difficulty in the a posteriori error control is called reliability-efficiency gap in [CJ03] and is caused by the degenerate convexity typically encountered in relaxed variational problems in the effective modelling of microstructures.

1.3.2.4 MARK and REFINE

Suppose that all element contributions $(\eta_\ell^2(T) : T \in \mathcal{T}_\ell)$ defined in the previous subsection are known on the current level ℓ with triangulation \mathcal{T}_ℓ . Given the input parameter $\Theta \in (0, 1)$ select a subset \mathcal{M}_ℓ of \mathcal{T}_ℓ (of minimal cardinality) with

$$\Theta \eta_\ell^2 \leq \sum_{T \in \mathcal{M}_\ell} \eta_\ell^2(T) =: \eta_\ell^2(\mathcal{M}_\ell). \quad (1.10)$$

This selection condition is also called *bulk criterion* or Dörfler marking [Dör96, MNS02] and is easily arranged with some greedy algorithm.

Any marked element is bisected according to the rules in Figure 1.1 and further mesh refinements may be necessary (e.g., via newest vertex bisection) such that $\mathcal{T}_{\ell+1}$ is a refinement of \mathcal{T}_ℓ with $\mathcal{M}_\ell \subset \mathcal{T}_\ell \setminus \mathcal{T}_{\ell+1}$.

Theorem 1.3.2 does not need the refinement with five bisections to obtain the interior node property and may focus on green-blue-red or green-blue refinement strategies.

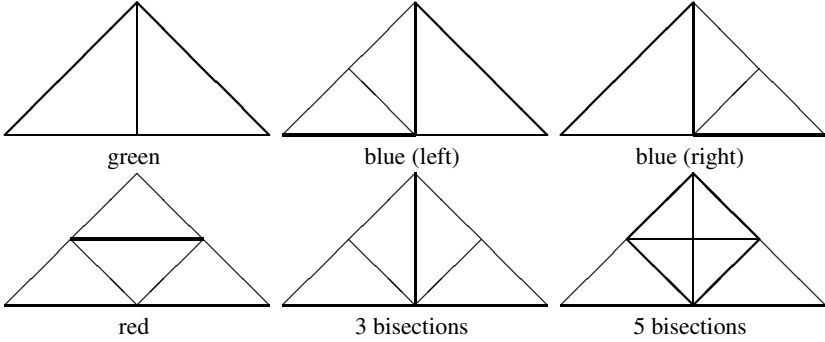


Fig. 1.1 Possible refinements of a triangle (up to rotations)

1.3.2.5 OUTPUT and Convergence Result

For a given triangulation \mathcal{T}_ℓ the adaptive scheme generates the triangulation at the next level $\mathcal{T}_{\ell+1}$ by a successive completion of the subroutines

$$\text{SOLVE} \rightarrow \text{ESTIMATE} \rightarrow \text{MARK} \rightarrow \text{REFINE} \quad (1.11)$$

Based on the input triangulation \mathcal{T}_0 , this scheme defines a sequence of meshes $\mathcal{T}_0, \mathcal{T}_1, \mathcal{T}_2, \dots$ and associated discrete subspaces

$$V^{(0)} \subsetneq V^{(1)} \subsetneq \dots \subsetneq V^{(\ell)} \subsetneq V^{(\ell+1)} \subsetneq \dots \subsetneq V = H^1(\Omega; \mathbb{R}^2) \quad (1.12)$$

with discrete minimizers $u_\ell \in u_D + V_0^{(\ell)}$, $\ell \in \mathbb{N}_0$. The main properties of this sequence of solutions are formulated in Theorem 1.3.1 and Theorem 1.3.2.

1.3.3 Convergence for the Deformation Gradient

The first main result of [CD14] shows strong convergence for three out of four components in the deformation gradient. The fact that the last component cannot be controlled is related to the degenerate convexity of the relaxed energy.

Theorem 1.3.1. *Let $u \in \mathcal{A}$ be a minimizer of I^{qc} , and let u_h be a minimizer of I^{qc} in a finite element space $u_D + V_{h,0}$ with $u_D \in V_h$ and Courant finite element method with respect to some shape-regular triangulation \mathcal{T}_h . Then there exist constants C_1 and C_2 which depend on the triangulation only through the shape-regularity such that, in a suitable coordinate system with $A_1 - A_2 = \text{diag}(\eta_1, \eta_2)$,*

$$\begin{aligned} & \|\partial_1(u - u_h)_1\|_{H^{-1}(\Omega)} + \sum_{j,k=1,2; (j,k) \neq (1,1)} \|\partial_k(u - u_h)_j\| \\ & \leq C_1 \min_{v_h \in u_D + V_{h,0}} (I^{\text{qc}}(v_h) - I^{\text{qc}}(u)). \end{aligned}$$

If $u \in H^2(\Omega; \mathbb{R}^2)$ then

$$\min_{v_h \in u_D + V_{h,0}} (I^{\text{qc}}(v_h) - I^{\text{qc}}(u)) \leq C_2 h \|D^2 u\|.$$

The second main result of [CD14] guarantees the convergence of the adaptive mesh-refining process of 1.3.2.

Theorem 1.3.2. *Suppose that the assumptions in Theorem 1.3.1 hold. Then the sequence $(u_\ell)_{\ell \in \mathbb{N}}$ with $u_\ell \in u_D + V_0^{(\ell)}$, $\ell \in \mathbb{N}_0$, computed by the adaptive scheme converges with respect to the weak topology of $H^1(\Omega; \mathbb{R}^2)$ to the unique minimizer u of the variational integral I^{qc} in the class of admissible functions \mathcal{A} . Moreover, the energies $I^{\text{qc}}(u_\ell)$ converge, i.e.,*

$$\lim_{\ell \rightarrow \infty} I^{\text{qc}}(u_\ell) = I^{\text{qc}}(u) = \min_{v \in u_D + H_0^1(\Omega; \mathbb{R}^2)} I^{\text{qc}}(v),$$

and, in a suitable coordinate system with $A_1 - A_2 = \text{diag}(\eta_1, \eta_2)$, all components of the deformation gradient except the $(1, 1)$ -component converge strongly $L^2(\Omega)$, i.e.,

$$\|\partial_1(u - u_\ell)_1\|_{H^{-1}(\Omega)} + \sum_{j,k=1,2; (j,k) \neq (1,1)} \|\partial_k(u - u_\ell)_j\| \rightarrow 0 \text{ as } \ell \rightarrow \infty.$$

One key ingredient in the proof is the observation [Koh91] that the relaxation of the energy (1.4) can be written as the sum of a convex and a polyaffine function which in the case at hand is a multiple of the determinant. This special structure has, e.g., been used in [Ser96, Ser98] to obtain uniqueness results and regularity of phase boundaries while our approach is in the spirit of the translation method which has been widely used in homogenization theory to separate nonconvex terms with special structure, usually polyaffine functions, from others terms. The key lemma of [CD14] reads as follows.

Lemma 1.3.3 (convexity control). *There exists some matrix \mathbf{D} with the maximal eigenvalue $\rho(\mathbf{D})$ such that the constant $\lambda_1 := \max\{1/(4(\gamma_1^2 + \gamma_2^2)), 4\rho(\mathbf{D})\}$ satisfies*

$$\lambda_1 |D\Phi(A) - D\Phi(B)|^2 \leq \Phi(A) - \Phi(B) - D\Phi(B) : (A - B) \quad \text{for all } A, B \in \mathbb{M}.$$

Proof. The proof in [CD14, Theorem 4.1] leads to the existence of the constant λ_1 . The matrix \mathbf{D} and the new explicit expression of λ_1 are derived in the appendix of this paper. \square

1.4 Guaranteed Lower Energy Bounds for the Two-Well Problem

The conforming finite element method from the previous section leads to upper energy bounds. This section discusses the computation of guaranteed lower energy bounds with nonconforming finite elements.

1.4.1 Nonconforming FEM and Discrete Energy Functional

The nonconforming P_1 finite element space (also named after Couzeix-Raviart) is defined by

$$\text{CR}^1(\mathcal{T}) := \{v \in P_1(\mathcal{T}) \mid v \text{ is continuous in the interior edges' midpoints}\}.$$

The space of nonconforming finite element functions that vanish in the boundary edges' midpoints is denoted by

$$\text{CR}_0^1(\mathcal{T}) := \{v \in \text{CR}^1(\mathcal{T}) \mid v \text{ vanishes in the boundary edges' midpoints}\}.$$

Set

$$\text{CR}^1(\mathcal{T}; \mathbb{R}^2) := [\text{CR}^1(\mathcal{T})]^2 \quad \text{and} \quad \text{CR}_0^1(\mathcal{T}; \mathbb{R}^2) := [\text{CR}_0^1(\mathcal{T})]^2.$$

For a triangle T , the Crouzeix-Raviart interpolation $I_{\text{CR}} : H^1(T) \rightarrow P_1(T)$ acts on $v \in H^1(T)$ through

$$I_{\text{CR}}v(\text{mid}(F)) = \oint_F v ds \quad \text{for all } F \in \mathcal{F}(T)$$

and enjoys the integral mean property of the gradient

$$\nabla I_{\text{CR}}v = \oint_T \nabla v dx. \quad (1.13)$$

The following approximation property of I_{CR} with the constant $\varkappa := \sqrt{1/48 + j_{1,1}^{-2}} = 0.298234942888$ is proven in [CG14].

Proposition 1.4.1 (Thm. 4 of [CG14]). *For any $v \in H^1(T)$ on a triangle T the Crouzeix-Raviart interpolation operator satisfies*

$$\|v - I_{\text{CR}}v\|_{L^2(T)} \leq \varkappa h_T \|\nabla(v - I_{\text{CR}}v)\|_{L^2(T)}. \quad \square$$

It is well-known that the classical nonconforming P_1 FEM may be unstable for problems involving the linearized Green strain tensor due to the lack of a discrete Korn inequality. Indeed, the nonconforming FEM allows for configurations with piecewise (infinitesimal) rigid body motions $v_h \in \text{CR}_0^1(\mathcal{T})$ such that $D_{\text{NC}}v_h$ is a nonzero skew-symmetric matrix field. The technique from [HL03] employs, with some positive parameter α , the stabilization term

$$\alpha \sum_{F \in \mathcal{F}} \oint_F |[v_h]_F|^2 ds.$$

The following discrete Korn inequality is proven in [HL03].

Proposition 1.4.2 (Proposition 2.2 of [HL03]). *For any $\alpha > 0$ there exists a positive constant $C(\alpha)$ which only depends on the shape-regularity in \mathcal{T} such that any $v_h \in \text{CR}^1(\mathcal{T})$ satisfies*

$$C(\alpha)^{-1} \|D_{\text{NC}}v_h\|^2 \leq \|\varepsilon_{\text{NC}}(v_h)\|^2 + \alpha \sum_{F \in \mathcal{F}} \oint_F |[v_h]_F|^2 ds. \quad \square$$

The discrete convex energy functional reads (for all $v_h \in \text{CR}^1(\mathcal{T}; \mathbb{R}^2)$)

$$E_{\text{NC}}(v_h) := \int_{\Omega} \Phi(D_{\text{NC}}v_h) dx + \alpha \sum_{F \in \mathcal{F}} \oint_F |[v_h]_F|^2 dx - \int_{\Omega} f \cdot v_h ds.$$

The discrete set of admissible functions reads

$$\mathcal{A}_{\text{CR}} := I_{\text{CR}}u_D + \text{CR}_0^1(\mathcal{T}; \mathbb{R}^2)$$

and gives rise to the discrete problem

$$u_h \in \arg \min_{v_h \in \mathcal{A}_{\text{NC}}} E_{\text{NC}}(v_h).$$

Note that super-linear growth of E_{NC} (and thus well-posedness of the minimization problem) follows with Lemma 1.4.3 below provided $\alpha > 0$ is sufficiently large (dependent on γ). This restriction on α is required because the term in (1.9) involves the determinant of quadratic growth.

1.4.2 Lower Energy Bounds

Let $C_{\text{ell}} = 2 \min\{\mu, \kappa\}$ denote the ellipticity constant that satisfies

$$C_{\text{ell}}|E|^2 \leq |E|_{\mathbb{C}}^2 := E : CE \quad \text{for any } E \in \mathbb{S}. \quad (1.14)$$

Lemma 1.4.3 (growth condition). *The constants $C_1 := 2/C_{\text{ell}} = \max\{1/\mu, 1/\kappa\}$ and $C_2 := C_1 (\max\{|A_1|_{\mathbb{C}}, |A_2|_{\mathbb{C}}\} - \min\{w_1, w_2 - g/2\})$ satisfy, for any $E \in \mathbb{S}$, that*

$$|E|^2 \leq C_1 W^{\text{qc}}(E) + C_2.$$

Proof. Let $E \in \mathbb{S}$. In case that $E \in \mathcal{P}_{\text{rel}}$, the definition of \mathcal{P}_{rel} yields $|W_1(E) - W_2(E)| \leq g/2$ and, hence,

$$\frac{1}{2g}(W_2(E) - W_1(E) + g/2)^2 \leq g/2. \quad (1.15)$$

For any $j = 1, 2$, the Young inequality reads

$$\frac{1}{2}|E|_{\mathbb{C}}^2 - |A_j|_{\mathbb{C}}^2 \leq |E - A_j|_{\mathbb{C}}^2. \quad (1.16)$$

The combination of (1.15)–(1.16) with the definition of W^{qc} from (1.6) results in

$$\frac{1}{2}|E|_{\mathbb{C}}^2 - \max\{|A_1|_{\mathbb{C}}, |A_2|_{\mathbb{C}}\} + \min\{w_1, w_2 - g/2\} \leq W^{\text{qc}}(E).$$

The ellipticity (1.14) and elementary algebra conclude the proof. \square

Lemma 1.4.4 (Korn-type inequality). *Any $v \in \mathcal{A}$ satisfies*

$$\|Dv\|^2 \leq 4\|\varepsilon(v)\|^2 + 5\|Du_D\|^2. \quad (1.17)$$

Proof. The Korn inequality

$$\|Dv\|^2 \leq 2\|\varepsilon(v)\|^2 \quad \text{for any } v \in H_0^1(\Omega; \mathbb{R}^2)$$

is an elementary consequence of the integration by parts formula. For a general function $v \in A$, the split $v = v_0 + v_D$ into $v_0 \in H_0^1(\Omega; \mathbb{R}^2)$ and the harmonic extension $v_D \in \mathcal{A}$ of the Dirichlet data $u_D|_{\partial\Omega}$ leads to

$$\|Dv\|^2 \leq 2\|\varepsilon(v_0)\|^2 + \|Dv_D\|^2.$$

The Young inequality $4ab \leq a^2 + 4b^2$ for any $(a, b) \in \mathbb{R}^2$ implies

$$0 \leq \|\varepsilon(v_0)\|^2 + 4\|\varepsilon(v_D)\|^2 + 4(\varepsilon(v_0), \varepsilon(v_D))_{L^2(\Omega)}.$$

Therefore,

$$\frac{1}{2}\|\varepsilon(v_0)\|^2 \leq \|\varepsilon(v_0)\|^2 + 2\|\varepsilon(v_D)\|^2 + 2(\varepsilon(v_0), \varepsilon(v_D))_{L^2(\Omega)} = \|\varepsilon(v)\|^2 + \|\varepsilon(v_D)\|^2.$$

Hence, the elementary estimate $\|\varepsilon(v_D)\| \leq \|D(v_D)\|$ leads to

$$\|Dv\|^2 \leq 4\|\varepsilon(v)\|^2 + 5\|Dv_D\|^2.$$

Since the harmonic extension v_D minimizes the H^1 seminorm subject to the boundary conditions $u_D|_{\partial\Omega}$, any other extension $u_D \in \mathcal{A}$ provides the upper bound $\|Dv_D\| \leq \|Du_D\|$. This proves (1.17). \square

Lemma 1.4.5. *With the Friedrichs constant C_F , the constants C_1, C_2 from Lemma 1.4.3, and γ from (1.8), any $v \in \mathcal{A}$ satisfies*

$$\|Dv\|^2 \leq 8C_1E(v) + 8\gamma C_1 \int_{\Omega} \det Dv \, dx + 8|\Omega|C_2 + 16C_1^2C_F^2\|f\|^2 + 5\|u_D\|^2.$$

Proof. The Korn-type estimate (1.17), Lemma 1.4.3 and the definition of E imply

$$\begin{aligned} \|\varepsilon(v)\|^2 &\leq C_1 \int_{\Omega} W^{\text{qc}}(\varepsilon(v)) \, dx + \int_{\Omega} C_2 \, dx \\ &= C_1E(v) + C_1 \int_{\Omega} f \cdot v \, dx + C_1\gamma \int_{\Omega} \det Du \, dx + \int_{\Omega} C_2 \, dx. \end{aligned}$$

The Friedrichs inequality with constant C_F and the Young inequality prove

$$\begin{aligned} C_1 \int_{\Omega} f \cdot v \, dx &\leq C_1\|f\| \|v\| \\ &\leq C_1C_F\|f\| \|Dv\| \leq 2C_1^2C_F^2\|f\|^2 + \frac{1}{8}\|Dv\|^2. \end{aligned}$$

The combination of the foregoing displayed formulas proves the result. \square

Lemma 1.4.6. *It holds*

$$\begin{aligned} &\lambda_1 \|D\Phi(Du) - D\Phi(D_{\text{NC}}I_{\text{CR}}u)\|^2 + E_{\text{NC}}(u_h) \\ &\leq E(u) + \varkappa \|h_{\mathcal{T}}f\| \|(1 - \Pi_0)Du\| + \alpha \sum_{F \in \mathcal{F}} \int_F |[I_{\text{CR}}u]_F|^2 \, dx. \end{aligned}$$

Proof. The discrete problem shows that

$$\begin{aligned}
 E_{\text{NC}}(u_h) &= \min_{v_h \in \mathcal{A}_{\text{CR}}} E_{\text{NC}}(D_{\text{NC}} v_h) \\
 &\leq E_{\text{NC}}(I_{\text{CR}} u) \\
 &= \sum_{T \in \mathcal{T}} \int_T \Phi(D_{\text{NC}} I_{\text{CR}} u) dx + \alpha \sum_{F \in \mathcal{F}} \int_F |[I_{\text{CR}} u]_F|^2 dx - \int_{\Omega} f \cdot I_{\text{CR}} u dx.
 \end{aligned} \tag{1.18}$$

Lemma 1.3.3 for $A := Du$ and $B := I_{\text{CR}} u$ and an integration over $T \in \mathcal{T}$ lead to

$$\begin{aligned}
 \lambda_1 \|D\Phi(Du) - D\Phi(DI_{\text{CR}} u)\|_{L^2(T)}^2 &+ \int_T \Phi(DI_{\text{CR}} u) dx \\
 &\leq \int_T \Phi(Du) dx + \int_T D\Phi(DI_{\text{CR}} u) : D(u - I_{\text{CR}} u) dx.
 \end{aligned}$$

Since $D\Phi(DI_{\text{CR}} u)$ is constant on T , the projection property (1.13) shows that the last term on the right-hand side vanishes. This, (1.18), and Proposition 1.4.1 lead to

$$\begin{aligned}
 \lambda_1 \|D\Phi(Du) - D\Phi(D_{\text{NC}} I_{\text{CR}} u)\|^2 &+ E_{\text{NC}}(u_h) \\
 &\leq \int_{\Omega} \Phi(D_{\text{NC}} I_{\text{CR}} u) dx + \alpha \sum_{F \in \mathcal{F}} \int_F |[I_{\text{CR}} u]_F|^2 dx - \int_{\Omega} f \cdot I_{\text{CR}} u dx \\
 &= E(u) + \alpha \sum_{F \in \mathcal{F}} \int_F |[I_{\text{CR}} u]_F|^2 dx + \int_{\Omega} f \cdot (u - I_{\text{CR}} u) dx \\
 &\leq E(u) + \varkappa \|h_{\mathcal{T}} f\| \|(1 - \Pi_0)Du\| + \alpha \sum_{F \in \mathcal{F}} \int_F |[I_{\text{CR}} u]_F|^2 dx. \quad \square
 \end{aligned}$$

Let $C_{\text{sr}} := \max_{T \in \mathcal{T}} h_T^2 / |T|$ be the shape-regularity constant.

Theorem 1.4.7 (guaranteed lower energy bound). Any $v \in \mathcal{A}$ and

$$C(f, v) := \left(8C_1 E(v) + 8\gamma C_1 \int_{\Omega} \det Dv dx + 8|\Omega|C_2 + 16C_1^2 C_F^2 \|f\|^2 + 5\|u_D\|^2 \right)^{1/2}$$

satisfy

$$E_{\text{NC}}(u_h) \leq E(u) + C(f, v)(\varkappa \|h_{\mathcal{T}} f\| + 3\alpha C_{\text{sr}} / \pi^2).$$

Proof. For any $v \in \mathcal{A}$, the term $\int_{\Omega} \det Dv dx$ does not depend on the particular choice of v but only depends on the boundary data u_D . Hence, the combination of Lemma 1.4.5–1.4.6 leads to

$$E_{\text{NC}}(u_h) \leq E(u) + \varkappa \|h_{\mathcal{T}} f\| C(f, v) + \alpha \sum_{F \in \mathcal{F}} \int_F |[I_{\text{CR}} u]_F|^2 ds.$$

For any edge $F \in \mathcal{F}$, the Poincaré inequality along F and the trace inequality [DE12, eqn (1.42)] reveal for the edge patch ω_F that

$$\int_F |[I_{\text{CR}}u]_F|^2 dx \leq \pi^{-2} h_F \|\partial [I_{\text{CR}}u]_F / \partial s\|_{L^2(F)}^2 \leq \pi^{-2} C_{\text{sr}} \|D_{\text{NC}} I_{\text{CR}}u\|_{L^2(\omega_F)}^2.$$

The sum over all edges in \mathcal{F} and Lemma 1.4.5 conclude the proof. \square

Remark 1.4.8. The efficiency of the lower bound is topic of ongoing research. In particular, the requirement of a sufficiently large stabilization parameter α leads to an additive shift in the lower bound. The numerical tests below will investigate the dependence for a model situation.

1.4.3 Guaranteed Error Control for the Pseudo-stress

This section presents an application to guaranteed a posteriori error estimates for the pseudo-stress. Let $\tau := D\Phi(Du)$ and $\tau_h := D\Phi(D_{\text{NC}}u_h)$ denote the exact and discrete pseudo-stress.

The computable a posteriori error estimator for $\|\tau - \tau_h\|$ utilizes the conforming companion operator $J_3 : \text{CR}^1(\mathcal{T}) \rightarrow P_3(\mathcal{T}) \cap H^1(\Omega)$ from [CS15, Lemma 3.3] which satisfies, for any $v_h \in \text{CR}^1(T)$ and any $T \in \mathcal{T}$, that

$$\int_T (v_h - J_3 v_h) dx = 0 \quad \text{and} \quad \int_T D_{\text{NC}}(v_h - J_3 v_h) dx = 0.$$

Proposition 1.4.9 (guaranteed a posteriori error estimate). *The exact minimizer $u \in \mathcal{A}$ of E and its pseudo-stress $\tau := D\Phi(Du)$ and the discrete minimizer u_h of E_{NC} with discrete pseudo-stress $\tau_h := D\Phi(D_{\text{NC}}u_h)$ satisfy*

$$\lambda_1 \|\tau - \tau_h\|^2 \leq 2 \left(E_{\text{NC}}(u_h) - E(u) + \int_{\Omega} f \cdot (u_h - J_3 u_h) dx \right) + \frac{1}{\lambda_1} \|D_{\text{NC}}(u_h - J_3 u_h)\|^2.$$

Proof. The convexity control from Lemma 1.3.3 for $A := D_{\text{NC}}u_h$ and $B := Du$ and an integration over Ω lead to

$$\begin{aligned} \lambda_1 \|\tau - \tau_h\|^2 &\leq \int_{\Omega} \Phi(D_{\text{NC}}u_h) dx - \int_{\Omega} \Phi(Du) dx - \int_{\Omega} \tau : D_{\text{NC}}(u_h - u) dx \\ &= E_{\text{NC}}(u_h) - E(u) + \int_{\Omega} f \cdot (u_h - u) dx - \int_{\Omega} \tau : D_{\text{NC}}(u_h - u) dx. \end{aligned}$$

The projection property of the companion operator J_3 and the discrete Euler-Lagrange equation reveal

$$\int_{\Omega} \tau : D_{\text{NC}}(u_h - u) dx = \int_{\Omega} (1 - \Pi_0) \tau : D_{\text{NC}}(u_h - J_3 u_h) dx + \int_{\Omega} f \cdot (J_3 u_h - u) dx.$$